Mechanics of Materials 41 (2009) 252–260

Contents lists available at ScienceDirect

Mechanics of Materials

journal homepage: www.elsevier.com/locate/mechmat

Dynamic split tensile test of Flattened Brazilian Disc of rock with SHPB setup

Q.Z. Wang [a,b,*], W. Li [a], H.P. Xie [a]

[a] Department of Civil Engineering and Applied Mechanics, Sichuan University, Chengdu, Sichuan 610065, China
[b] State Key Laboratory of Hydraulics and Mountain River Engineering, Chengdu, Sichuan 610065, China

ARTICLE INFO

Article history:
Received 6 January 2008
Received in revised form 6 October 2008

ABSTRACT

The Flattened Brazilian Disc (FBD) specimens were impacted diametrically by a pulse shaping split Hopkinson pressure bar to measure dynamic tensile strength of a brittle rock. With application of strain gauge technique, the stress waves traveling through the incident bar, the transmission bar as well as the FBD specimen were recorded and analyzed. The loading history was determined based on the one-dimensional stress wave theory. The dynamic equilibrium condition in the specimen was approximately satisfied, this claim was supported by the numerical simulation of dynamic stress evolution in the specimen, with the conclusion that a short time after impact the pattern of dynamic stress distribution in the specimen was symmetric and similar to that of the counterpart static loading. The validity of the test was further verified experimentally, as the waveforms acting on the two flat ends of the FBD specimen, respectively, were of nearly the same shape, and the rupture modes of the specimens were generally such that crack first initiated at the center of the disc and subsequently propagated along the loading diameter, whereas crush zones were implied to form lastly near the two flat ends of the broken specimen. The dynamic tensile strength of marble was measured at the critical point when the tensile strain wave recorded at the disc center got peak value of the strain derivative with respect to time.

1. Introduction

The tensile strength of rock material is typically an order of magnitude smaller than the compressive strength, tensile failure often occurs in rock masses. In addition, in many rock related engineering projects, e.g. blast and fragmentation in mining and military operation, rock breakage is often affected by loading rate. Hence research on various methods to measure dynamic tensile strength of rock materials is important for application in geotechnical engineering and development in rock mechanics. However, a direct tension test of rock is very difficult to perform, so that an indirect tension, such as the Brazilian test, also called the split tensile test, has been a popular choice. International Society for Rock Mechanics (ISRM) issued the suggested method for testing static rock tensile strength with the Brazilian disc specimen (ISRM, 1978). American Society for Testing and Material also adopted a similar method for testing concrete (ASTM C496/C496M-04). The main drawback of the Brazilian test is that it is not easy to maintain an ideal contact between the platens of a test machine and the circular boundary of a disc specimen, and the stress concentration caused by the point load on the disc may bring about premature breakage of the specimen at the contact point. As the crack is not first initiated from the center of the disc as expected, the underlying principle of the Brazilian test is violated. In order to avoid this unreasonable failure mode of the disc specimen, a pair of rounded anvils has been adopted by many researchers, among them the early practitioners are Awaji and Sato (Awaji and Sato, 1979). However, the match between the anvils and the periphery of a disc specimen is

* Corresponding author. Address: Department of Civil Engineering and Applied Mechanics, Sichuan University, Chengdu, Sichuan 610065, China.
E-mail address: qzwang2004@163.com (Q.Z. Wang).

0167-6636/$ - see front matter © 2008 Elsevier Ltd. All rights reserved.
doi:10.1016/j.mechmat.2008.10.004

very complicated, it is difficult to determine an accurate contact width between the anvils and the disc (Awaji and Sato, 1979); and for discs of different diameters, differently sized anvils may be required to test them. Another solution to the problem was to machine two parallel flat ends on the disc circumference for appliance of a distributed load, then the regular complete disc was modified and became the Flattened Brazilian Disc (FBD) (Wang and Xing, 1999). We are just promoting the FBD specimen from the static test to the dynamic split tensile test (Wang et al., 2006). Being used in the dynamic test, the flat ends of the FBD specimen may be especially more convenient than the curved anvils or glued bearing strips proposed by ISRM and ASTM, as the anvils or strips may have a negative influence on the stress wave behavior in the dynamic Brazilian test.

The strain rate of rock fragmentation is usually in the range of 10^1–$10^4\ s^{-1}$, a split Hopkinson pressure bar (SHPB) setup is suitable for testing rock at such strain rates (Wang et al., 2006; Kolsky, 1949; Rodriguez et al., 1994; Buchar and Rolc, 2006; Gomez et al., 2001, 2002; Grantham et al., 2004; Frew et al., 2001; Pan et al., 2005). "Proper experiments need to be carefully designed and constructed to acquire accurate and reliable material properties" (Pan et al., 2005). Specifically wave propagation should be considered when studying the dynamic mechanical properties of materials at such high strain rates. For a comprehensive evaluation of the dynamic split test, attention was focused on three key aspects for the tested specimen (Rodriguez et al., 1994): the assumption of elastic behavior; the evolution history of stress distribution; and the failure mode. Dynamic split tests were reported recently for various materials including rocks, ceramics and an explosive simulant (Wang et al., 2006; Rodriguez et al., 1994; Buchar and Rolc, 2006; Gomez et al., 2001, 2002; Grantham et al., 2004). The test result for ceramics was shown to agree with result of the Taylor test in a comparison study (Buchar and Rolc, 2006). Especially worth mentioning is the photoelastic dynamic experiment using complete disc specimens performed by Gomez et al. (2001, 2002), they validated the dynamic split test by stating that "the photoelastic experiments determined that the specimens were in equilibrium, and the dynamic stress field resembled the static field." Another significant contribution to this topic is the high-rate experiment with an explosive simulant done by Grantham et al. (2004), they concluded that "The essential features of low-rate Brazilian tests are found to occur in the high-rate experiments, with the samples reaching equilibrium quickly and remaining in equilibrium throughout the experiment" (Grantham et al., 2004). In our study, differently sized FBD specimens of marble were diametrically impacted at the flat end by SHPB with varied impact speeds. In order to obtain an ideal loading wave, a thin aluminum circular plate was glued on the end surface of the incident bar as a pulse shaper for the incident wave, the pulse shaper was stricken by the projectile. A numerical simulation using finite element method was performed to show the evolution of dynamic stress distribution in various specimens. The results indicate that at a certain stage of time, i.e., after several reverberation of stress wave in the specimen, similar to that of the counterpart static test, a symmetric pattern of stress between left end and right end of the specimen is reached. Besides that, according to the stress waves recorded on the incident bar and the transmission bar respectively, the forces acting on the two flat ends of the FBD specimen are nearly equal, thus dynamic equilibrium is further shown experimentally. The splitting rupture mode of the FBD specimens is observed: center crack initiation and crack propagation along the loading diameter. The measured dynamic tensile strength of marble shows strain rate effect as compared with the counterpart static value.

2. SHPB setup and specimen preparation

A FBD specimen located between the bars of a SHPB setup is sketched in Fig. 1, the incident bar with a pulse shaper is to be stricken by the projectile. The loading manner for the specimen is shown in Fig. 2, a distributed load on the two parallel flat ends substantially reduces the stress concentration, as compared to the regular complete disc subjected to concentrated loading. An appropriate flat end angle 2α, also called loading angle, may essentially guarantee crack initiation at the center of the disc, this conclusion is drawn based on our previous test experience and theoretical analysis with the FBD specimens (Wang and Xing, 1999; Wang et al., 2006; 2004; Wang and Wu, 2004), $2\alpha = 20^\circ$ was chosen for present investigation. P is the total value of the uniformly distributed load applied on the flat end.

In the previous study of FBD specimen for the static split tension test, Griffith strength criterion was used to

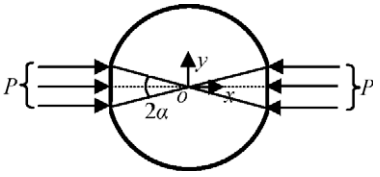

Fig. 2. Loading model for a FBD specimen.

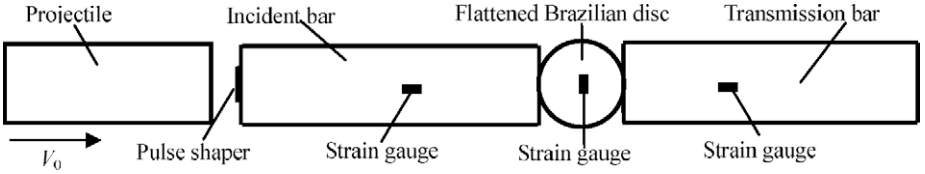

Fig. 1. Schematic diagram of a FBD specimen and SHPB setup.

formulate the calculation formula, where the contact conditions between the platens of test machine and the flat ends of the specimen were considered (Wang et al., 2004). For the loading angle $2\alpha = 20^\circ$ a formula for calculating tensile strength σ_t using FBD specimens is given as follows (Wang et al., 2004; Wang and Wu, 2004):

$$\sigma_t = -0.95\frac{2P_{\max}}{\pi DB} \quad (1)$$

where $P_{\max}$ is maximum load, D is diameter and B is thickness of specimen. Compressive stress is taken as positive in this paper, so negative normal stress represents tension.

The diameter of the bars in our SHPB setup is 100 mm, so the area of the end of the bar is large enough to cover the flat ends of a FBD specimen. The length of the incident bar is 4500 mm, the length of the transmission bar is 2500 mm. Material parameters for the bar are: elastic modulus 210 GPa, Poison's ratio 0.25–0.30, density 7850 kg/m^3. In order to record the incident wave, the reflected wave and the transmission wave, on both lateral sides of the incident bar and transmission bar are attached strain gauges, for the incident bar the location of the strain gauge is 1495 mm to the side contacting the specimen's left end, for the transmission bar the location is 190 mm to the side contacting the specimen's right end. 190 mm is long enough to avoid the boundary effect; and for the incident bar 1495 mm is also long enough to separate the incident wave and the reflected wave. The strain gauge location of the bars ensures that the uniformity of axial stress is achieved over the entire cross section of the bars. The length of the projectile is 500 mm, the longer the projectile, the longer the loading duration, which makes it easier to realize dynamic stress equilibrium and maintain the equilibrium status up to specimen failure (Gomez et al., 2001). The tested material was a white marble taken from Ya'an city, Sichuan province, with a Poisson's ratio of 0.3, an elastic modulus of 1.6×10^4 MPa, and a density of 2527 kg/m^3. There were five types of specimens, including 19 specimens of type A (diameter $\times$ thickness: Φ 65 mm $\times$ 26 mm) for studying strain rate effect, 4 of type B (Φ 75 mm $\times$ 30 mm), 4 of type C (Φ 85 mm$\times$34 mm), 3 of type D (Φ 85 mm $\times$ 30 mm), 5 of type E (Φ 65 mm $\times$ 30 mm).

Marble is a brittle material, its tensile strength is low, usually it fails promptly at a small strain. Under high strain rate loading, if the loading waveform is not properly designed, the specimen may break at a moment when the incident wave is still rising and the stress equilibrium has not been reached. To solve this crucial problem, a thin circular aluminum plate (Φ 45 mm $\times$ 1 mm) is glued co-centrically at the impacted end of the incident bar, this end is to be stricken by the projectile (Fig. 1). This pulse shaper makes the rising front of the pulse not so steep, which will be shown in more detail in Section 3.1 of this paper. The pulse shaper makes the wave to have enough time to reverberate to-and-fro in the specimen, and this ideal triangular waveform makes possible to produce a nearly uniform distribution of the stress in the specimen after a certain time (Frew et al., 2005). In contrast, if a rectangular wave is used, the sharply rising and oscillating stress wave may surpass the strength limit very soon and destroy the specimen at the very initial stage of impact, this is the reason why the rectangular waveform is not suitable for loading marble specimens. In Fig. A1 in the Appendix, three recorded incident waveforms in a preliminary experiment before the normal test are given, the comparison of the differences between these three waveforms demonstrates the role of the aluminum wave shaper which we adopted in our experimental study. The triangular stress wave is also an ideal waveform in dynamic test to reduce the dispersion effect.

Fig. 3 is a photo showing a FBD specimen being placed between the incident bar and the transmission bar before actual impact, the parallelism of the two flat ends of the FBD specimen is important and hence should be checked carefully. Strain gauges are glued on the same location at both lateral plane sides of the disc and perpendicular to the loading direction, the average recording of the two strain gauges at two opposite sides is used. The strain gauges used in the current work have an electric resistance value of 120.0 ± 0.1 Ω, a sensitivity coefficient of 2.14 ± 1%, and a gauge length of 4.5 mm. Compared with the size of FBD specimens, the strain gauge glued at the surface of the specimen is very small and thin, so the effects of crack bridging to the splitting crack by the gauges and the glue can be neglected. The failure tensile strain is about 2000 με, which is much smaller than the failure compressive strain.

3. Experimental recordings and numerical results

3.1. Proof of test validity

With a thin circular aluminum plate glued co-centrically at the impact end of the incident bar (Fig. 1), the rising front of the incident wave, which is recorded by the strain gauge attached on the incident bar, is indeed prolonged. In Fig. A1 in the Appendix, the role of a aluminum wave shaper in shaping the waveform can be seen very clearly, as compared with a paper wave shaper and the case without shaper. In the formal experiment, as shown in Fig. 4(a) this smooth triangular waveform has a rising time length of about 260 μs, the rising front of the stress pulse is not steep, high frequency oscillating components disappear. Fig. 4(b) is the transmitted wave. Fig. 4(c) is the record of tensile strain history at the center of the specimen, the strain rate is the derivative of the strain with

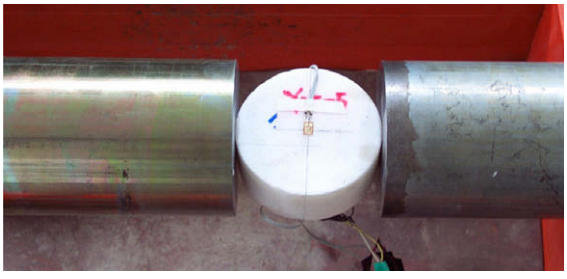

Fig. 3. Photo of a FBD specimen being placed between the bars before dynamic split test by SHPB.

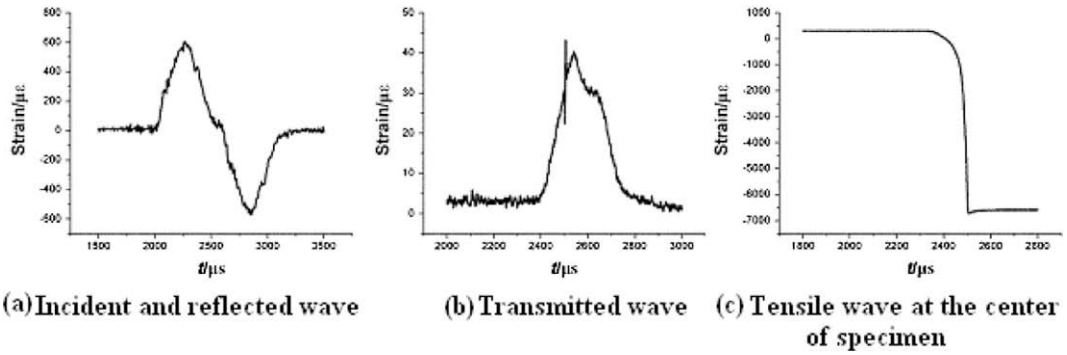

Fig. 4. Recordings of strain waves for testing specimen E30-5.

respect to time; however, only the intermediate curve is useful, actually the specimen fails in this section. The bottom horizontal line shows a cut-off for the measurement range of strain and is hence of no use. For the intermediate curve, beginning from zero, the absolute value of this derivative increases with increment of time t, and upon reaching the peak value with minor oscillations, it abruptly drops to zero again, so the shape of strain rate history is like a spike. The failure starts from crack initiation at the disc center, it corresponds to peak value of the strain rate, which is called failure strain rate or simply strain rate hereafter. It is interesting to note that Fig. 3 of Ref. (Grantham et al., 2004), if turned over up-side-down, is similar to our Fig. 4(c).

Rodriguez et al. gave out the history of dynamic stress distribution of the Brazilian disc (without flat ends) using finite element calculation and photoelastic experiment, respectively (Rodriguez et al., 1994), and the results of these two methods agreed favorably, this fact showed the effectiveness of modeling with dynamic finite element analysis. We checked the numerical work of Rodriguez et al. (1994) using ANSYS, a commercial finite element software, our result was essentially identical to that of Rodriguez et al. After this checkup, we did dynamic finite element analysis for dynamic stress distribution of the FBD specimens. In Fig. 5, the stress distributions of static loading are exactly symmetric, shown by the top left figure; for the remaining figures in Fig. 5 for the dynamic loading cases, after a certain time interval from the impact start, the stress distributions are approximately symmetric, indicating a status of dynamic stress equilibrium. Once the equilibrium state of the dynamic stress is reached in the specimen, the to-and-fro reflections of stress wave only increase the value of the stress, whereas the pattern of stress distribution is kept almost unchanged up to complete failure of the specimen (Gomez et al., 2001). It can be seen from Fig. 5 that, for different FBD specimens subjected to diametrical impact, the time needed to achieve dynamic equilibrium is not influenced by specimen thickness, it is mainly determined by specimen diameter, the larger the diameter, the longer the time needed to reach equilibrium. It should be pointed out that when the equilibrium is considered to be realized, the pattern of stress distribution in dynamic test is basically the same as that in the counterpart static test. However, minor difference occurs at the right end of the FBD as compared to the left end impacted by the incident bar. So, at dynamic equilibrium, based on such similarity of iso-stress contour pattern as compared with that of the static case, formula (1) can be used for calculation of dynamic tensile strength. In Fig. 5, the scales of the stresses are omitted for clarity and brevity, there is still some stress concentration at the conjunction point between the circular boundary and the flat end, where the iso-stress curves are concentrated. However, the stress concentration is largely reduced as compared with the counterpart complete disc specimen acted by point load.

The failure modes of the specimens should be investigated from two perspectives. First, the location of crack initiation, whether the failure is initiated from the center of the disc is of vital importance. Second, the route of crack propagation, whether the major failure path is along the loading diameter is also important. To check the reasonability for the failure mode, three strain gauges were glued for type B specimens, these three gauges were aligned along the loading diameter and placed in accordance with the tensile direction. A sketch of the locations for the three gauges is given in Fig. A2 in the Appendix. Typical strain recordings with specimen labeled B30-33 is shown in Table 1, where channel 1 and channel 3 recordings are the strain gauge signals at the left end and right end, respectively, with a distance of 1/4 diameter from the disc center, whereas channel 2 recording is the strain gauge signal at the disc center. It can be seen from Table 1 that the time to failure for channel 2 (center) is 509 μs, which is the smallest (left is 551 μs, right is 553 μs), thus crack initiation at the disc center is verified. Please note that only few specimens were stuck three strain gauges in the way mentioned above, for the remain majority of specimens only one strain gauge is stuck at the center of the disc. In Fig. 6 the rupture modes of various types of FBD specimens are shown, the upper left picture is from a trial test, the specimen was subjected to a relatively low impact speed, it shows two almost complete halves after test. The other pictures represent specimens impacted with higher speeds, they are all broken into nearly equal halves separated along the loading diameter, and triangular crush zones are implied to exist near the two flat ends of the specimen, the higher the impact speed, the larger the triangular crush zone, and the triangular crush zone is larger at

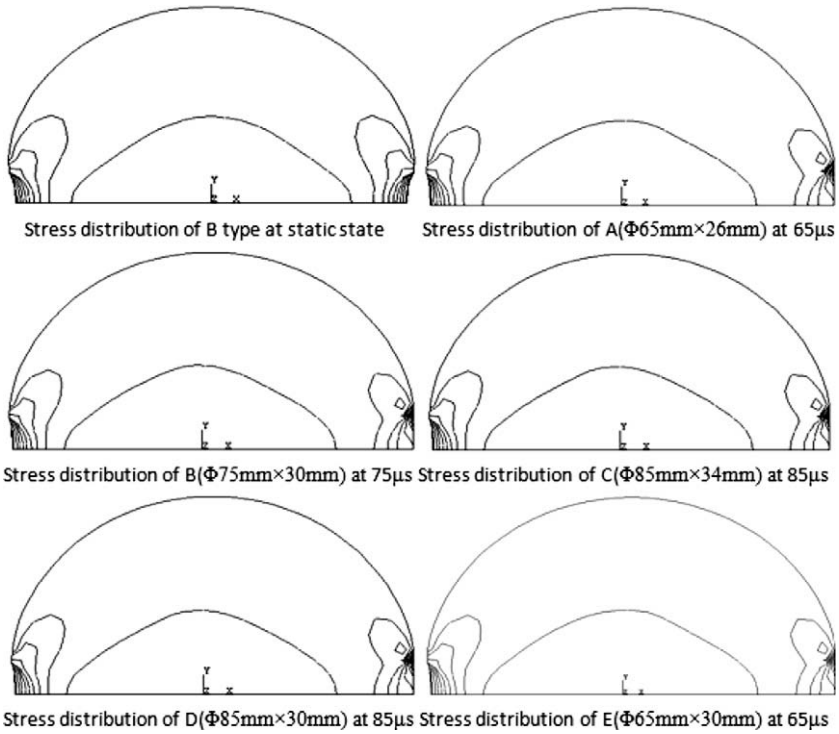

Fig. 5. The time to equilibrium and pattern of stress distribution for different FBD specimens (A–E) given out by finite element analysis.

Table 1
Strain history recordings for three stain gauges located along the diameter of B30-33 specimen.

Strain channel	Arriving time (μs)	Arriving strain amplitude (με)	Time to failure (μs)	Failure strain amplitude (με)	Time length of failure (μs)
1 (left)	256	658.8	557	1143.8	301
2 (center)	273	574.0	509	1574.5	236
3 (right)	291	634.7	553	2218.1	262

the impacted end of the specimen (marked with specimen label) stricken by the incident bar.

From the above observation and analysis it is shown that the assumption of elastic behavior is fundamentally reasonable for the dynamic split tension test of FBD specimens of marble impacted by SHPB. The crack is initiated from the center of the disc, and the crack propagates mostly along the loading diameter and towards the two flat ends, in this way the disc is broken into two halves, whereas the vacant regions near the two flat ends imply the existence of crush zones. However, the crush zones were formed after the crack initiation at the center and later propagation along the diameter, judged by the data on time sequence of strain gauge failure shown in Table 1. The validity of the dynamic Brazilian test is thus further justified experimentally.

3.2. Analysis of stress non-uniformity

In the process of wave propagation, the weakened region of rock specimen, such as micro cracks and voids, would reduce the amplitude of stress wave and resist wave propagation, as some energy is consumed through refraction and reflection. Furthermore, the density, the elastic modulus and wave speed of the specimen are all smaller than those of the pressure bars, wave reflection and transmission occur at the two flat ends. All these factors contribute to the stress non-uniformity at the two flat ends of the specimen. Table 2 presents experimental recordings of some typical specimens. It can be seen from Table 2 that the time non-uniformity does exist, and it should be taken into consideration in analyzing the recordings.

By stress non-uniformity we mean not only space non-uniformity but also time non-uniformity for stress wave. Space non-uniformity is related with amplitude variation, it shows the difference of the shape of the waves acting on the left end and right end of the specimen, respectively (Fig. 7). Time non-uniformity is referred to that the wave on the right end of the specimen lags somewhat behind the wave on the left end. Time non-uniformity is generated mainly by the relatively low wave impedance of the rock specimen as compared to the metal bars. Table 3 further shows the effect of projectile speed and specimen size to the non-uniformity of stress, where V_0 is the projectile

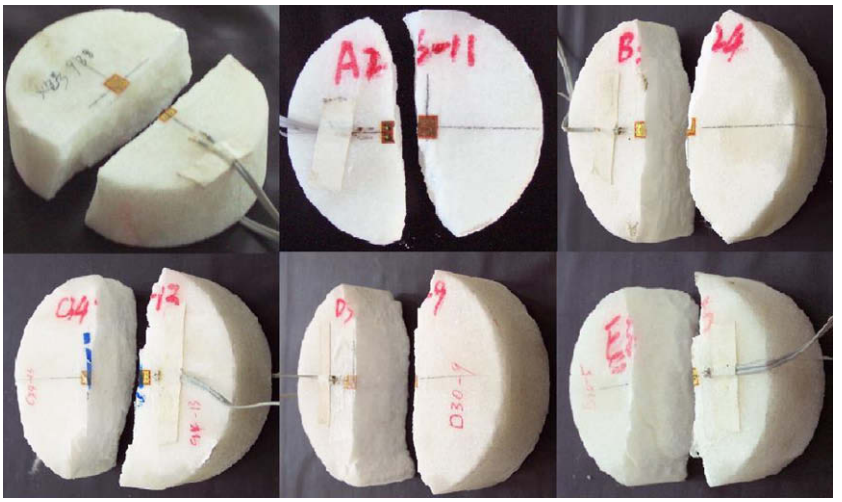

Fig. 6. Rupture modes of different types of FBD specimens.

Table 2
Recordings of strain waves for typical specimens.

Specimen	Incident wave				Reflected wave			
	Starting		Peak		Starting		Peak	
	Time (μs)	Strain (με)	Time (μs)	Strain (με)	Time (μs)	Strain (με)	Time (μs)	Strain (με)
A26-10	−44	87.2	264	594.4	532	135.8	860	−386.0
B30-24	−40	23.3	212	631.1	536	28.4	784	−543.8
C34-13	−44	−3.7	216	650.5	532	34.7	788	−635.1
D30-9	−44	8.7	236	588.2	532	47.6	804	−536.6
E30-5	−44	6.5	216	605.4	532	39.5	808	−566.6
Specimen	Transmitted wave						Non-uniformity time (μs)	Time length of failure (μs)
	Theoretical starting		Actual starting		Peak			
	Time (μs)	Strain (με)	Time (μs)	Strain (με)	Time (μs)	Strain (με)		
A26-10	284	−6.2	348	−7.2	552	36.8	64	204
B30-24	288	0.5	356	1.3	554	69.4	68	228
C34-13	284	−1.0	356	−1.2	568	9.8	72	212
D30-9	284	−2.0	356	−2.2	488	39.5	72	136
E30-5	284	3.1	344	3.5	492	39.7	60	148

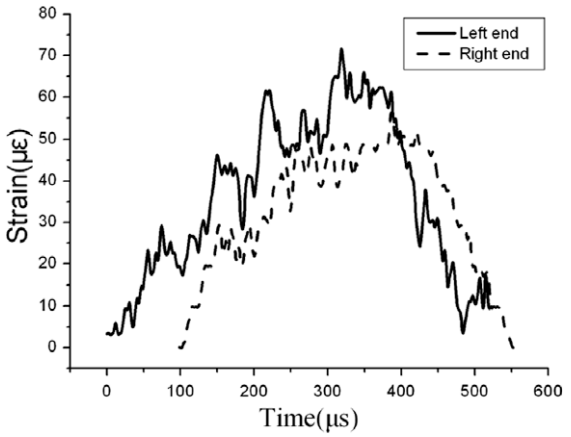

Fig. 7. Stress waves acting on the left end and right end of the FBD specimen respectively (Wang et al., 2006).

speed, T_i is the rising time length of incident wave, T_0 is the non-uniformity time, which is an indication of the time lag just mentioned above.

From Table 3 it can be seen that the time non-uniformity cannot be neglected as compared to the rising time length of the incident wave. It can also be seen that for the same type of specimens, the effect of impact speed to the time non-uniformity is marginal, the effect of thickness is also small, whereas the influence of specimen diameter is obvious, the larger the diameter, the larger the time non-uniformity. The stresses at the two flat ends are not strictly symmetric, therefore the three waves (incident, reflected, and transmitted) recorded on the pressure bars should be used to calculate the load in order to alleviate the effect of the space non-uniformity of stress.

In brief, the non-uniformity of stress makes the load on the left end and right end of the specimen different not

Table 3
A comparison of non-uniformity time for different types of FBD specimens.

Specimen	A26-10	A26-3	A26-19	A26-23	A26-21	B30-24	C34-13	D30-9	E30-5
V_0 (m s^{-1})	3.789	5.548	7.877	9.851	12.179	4.098	4.415	4.213	4.267
T_i (μs)	308	256	256	192	104	252	260	280	260
T_0 (μs)	64	56	60	52	60	68	72	72	60

only in the wave shape but also in the starting time, both non-uniformities are concerned with satisfaction of dynamic equilibrium. In treating the experimental data, calculation formula with time non-uniformity adjustment for the waves should be adopted. In the present paper, the left end of the specimen under test is taken as the starting point for the incident load appliance, so that the transmission wave $\varepsilon_t(t)$ should be translated towards the left along the abscissa, i.e. the time axis, in Fig. 4(b) with a time difference (time lag) of T_0 to get $\varepsilon_t^*(t)$, that is $\varepsilon_t^*(t)= \varepsilon_t(t+T_0)$, T_0 is given in Table 3, in this way, the effect of time non-uniformity to the results is considered. More than that, since three recorded waves are used for calculating the load, the space non-uniformity at two flat ends is also considered. The load, which is to be used in Eq. (1) for calculating the dynamic tensile strength, of the dynamic split test is given below (Gomez et al., 2001).

$$P(t) = \frac{EA}{2}[\varepsilon_i(t) + \varepsilon_r(t) + \varepsilon_t^*(t)]. \tag{2}$$

Although Eq. (1) was derived for quasi-static situation, from the results of finite element modeling (Fig. 5) it can be seen that after 65 μs, 75 μs and 85 μs from the impact start for specimen with different diameters, the distribution of dynamic stress is similar to that of static stress, and this similarity will not change with increment of the time. If specimen failure occurs after dynamic equilibrium is reached, then the stress state at the failure location and time may be almost the same to the stress state at the same location in a quasi-static test. Further, from Fig. 7 it can be seen that the forces acting on the left end and right end of the specimen respectively are approximately equal. Judged by these two aspects, using Eqs. (1) and (2) to calculate the dynamic tensile strength is justified. Fig. 7 is a recording of a FBD specimen with a diameter of 75.5 mm in a preliminary experiment. With decreasing diameter, the time delay of the force history acting on the right end with respect to the left end also decreases. This time delay is about 100 μs in Fig. 7.

The tensile strain rate at the center of the FBD specimen is the derivative of the tensile strain history $\varepsilon_s(t)$ with respect to the time using Fig. 4(c):

$$\dot{\varepsilon}(t) = \frac{d\varepsilon_s(t)}{dt}. \tag{3}$$

As mentioned in Section 3.1, in Fig. 4(c), only the middle segment sandwiched by the two horizontal lines is used, in the following text and tables we use $\dot{\varepsilon}$ to denote the failure strain rate, which is the peak value of the strain derivative with respect to time. The dynamic tensile strength of marble was measured at this critical point.

3.3. The effect of impact speed and specimen size

Strain rate in the specimen is a very important parameter to dynamic split tension test. Factors that influence the strain rate mainly include the specimen size and the projectile speed. Table 4 shows these factors and their effect, where D is specimen diameter, B is the thickness, $\dot{\varepsilon}$ is the tensile failure strain rate, t is time length of failure, σ_t is the dynamic tensile strength. It can be seen from Table 4 that, the impact speed of the projectile has a marked influence on the time length of failure for the specimen, the larger the impact speed, the shorter the time length of failure. The specimen size has little influence on the time length of failure. Table 4 also shows that the failure strain rate increases a little with larger thickness and smaller diameter of the specimen. However, it should be pointed out that the range of scale of the specimens in our present study is not wide enough to draw a general conclusion about the size effect. The influence of the impact speed to the strain rate is more complicated, primarily the strain rate will increase with the increment of impact speed, however as the speed reaches a specific value of about 6.7 m s^{-1}, the strain rate will no longer increase, it is kept at somewhat above 24 s^{-1}.

Marble is a brittle material similar to brittle ceramics, as pointed out by Gama et al. that "slow loading via a shaped

Table 4
The dynamic tensile strength of marble σ_t vs strain rate $\dot{\varepsilon}$ under different test conditions.

Specimen	V_0 (m s^{-1})	D (mm)	B (mm)	$\dot{\varepsilon}$ (s^{-1})	t (μs)	σ_t (MPa)
A26-10	3.789	64.8	26.0	21.53	204	22.14
A26-3	5.548	65.4	25.5	22.75	184	24.12
A26-18	6.749	66.0	26.0	24.30	176	26.57
A26-19	7.877	65.0	26.0	24.77	168	27.10
A26-23	9.851	65.0	26.0	24.63	160	26.80
A26-29	10.622	65.3	25.5	24.37	152	26.93
A26-21	12.179	65.4	25.8	24.35	136	27.56
B30-24	4.098	75.7	30.3	23.69	228	24.36
C34-13	4.415	85.0	34.1	26.70	212	26.88
D30-9	4.213	84.8	29.3	22.69	136	23.91
E30-5	4.267	66.2	29.5	24.39	148	27.39

Table 5
A comparison of dynamic tensile strength σ_t of marble at different strain rates $\dot{\varepsilon}$.

Specimen	D (mm)	B (mm)	$\dot{\varepsilon}$ (s^{-1})	σ_t (MPa)
A12	65.6	26.0	0.13	5.23
A26-10	64.8	26.0	21.53	22.14
A26-3	65.4	25.5	22.75	24.12
A26-18	66.0	26.0	24.3	26.57
A26-19	65.0	26.0	24.77	27.10
A13	75.0	30.3	0.11	4.47
B30-24	75.7	30.3	23.69	24.36
A16	84.9	34.0	0.10	6.04
C34-13	85.0	29.3	22.69	26.88

pulse is an essential condition in testing brittle ceramics" (Gama et al., 2004), our loading is relatively slow as compared with that of Grantham et al. (2004), however it is beneficial to validate our test. Another point on dynamic equilibrium is that "considering the stress wave reverberation, the initial nonequilibrium is as high as 200%; however, it exponentially decreases to about 10% in four reverberations in the specimen" (Gama et al., 2004). Figs. 4 and 5 show that there are enough time for the loading waves to allow such reverberations.

3.4. Comparison of dynamic tensile strength at different strain rates

The previous results under low strain rate tested with a hydro-electrical servo test machine of INSTRON 1342 type are given in Table 5 as a base for comparison, these results are represented by specimens labeled A12, A13 and A16, it can be seen that the tensile strength at high strain rate is 4.2–5.4 times that at low strain rate. The corresponding static value is $\sigma_t = 4.81$ MPa.

4. Concluding remarks

Based on the results of both experimental and numerical investigations, we present the following concluding remarks for the dynamic split tension test of marble using FBD specimens and SHPB setup:

(1) Stress non-uniformity exists both in time and in space, these two types of non-uniformities should be considered in the analysis. To handle the time non-uniformity, a method of shifting the transmission wave along the time coordinate is used. On the other hand, to consider the space non-uniformity, three stress waves recorded on the bars are used in an average sense to calculate the impact load on the specimen.
(2) The aluminum pulse shaper can produces a ramp-shaped pulse (Figs. 4 and A1) which contains almost no high frequency oscillations. A triangular waveform makes possible to produce a nearly uniform distribution of the stress in the specimen after a certain time and also to reduce the dispersion effect.
(3) The FBD specimen has some advantages over the traditional complete disc specimen in the dynamic splitting test, the test method described in this paper is relatively simple. The pulse shaper and strain gauge technique are effective and economic, as compared to the more expensive instrument and sophisticated technique such as high-speed photography used in conjunction with the speckle metrology (Grantham et al., 2004).
(4) The dynamic tensile strength of marble at the strain rate $\dot{\varepsilon}$ of about 22 s^{-1} to 25 s^{-1} is around 22–27 MPa, the dynamic tensile strength is substantially higher than the corresponding static value, the latter is about 5 MPa.

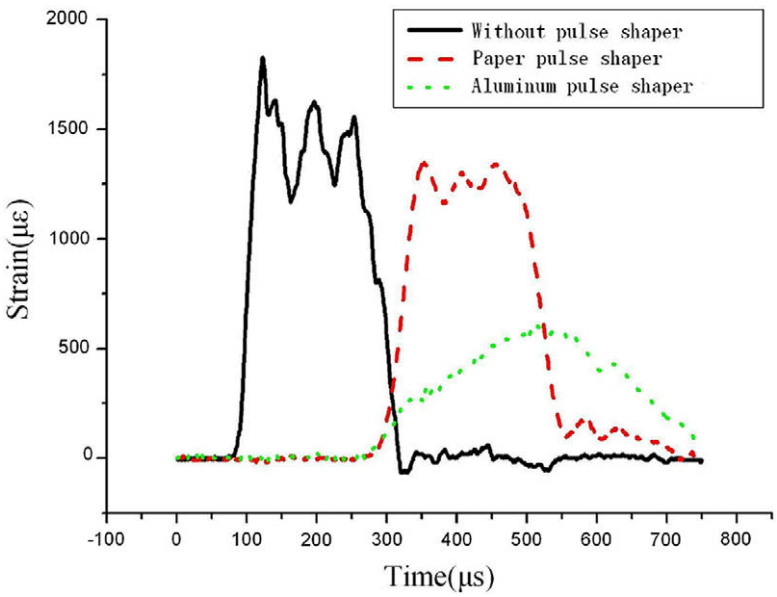

Fig. A1. A comparison of different incident waveforms shaped by different wave shapers, respectively.

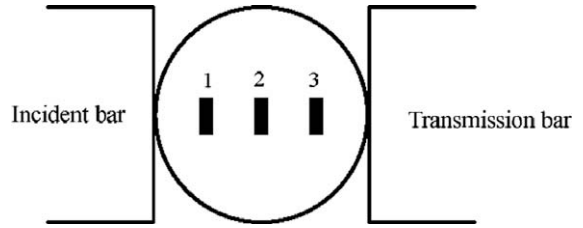

Fig. A2. A sketch of the three strain gauges attached on the loading diameter of a disc specimen to check the reasonability for the failure mode based on the sequence of the gauge breakage.

(5) Size effect on the dynamic tensile strength is mainly caused by the fracture process zone (FPZ) ahead of the crack tip, so that the relative length of the FPZ as compared to the disc diameter is crucial to it. The range of scale of the specimens in our present study is not wide enough to draw a solid conclusion on size effect. If the size of the tested specimen is large, then the FPZ can be neglected, the test result is the true material property, and if the specimen is not large enough, the tentative test values can be used to predict the true material value according to the size effect law. Another difficulty is that the dynamic size effect may also be influenced by time factor. Our research in this aspect is still ongoing.

Acknowledgements

This work was supported by the National Natural Science Foundation of China (projects Nos. 10472075 and 50490272), the State Key Laboratory of Hydraulics and Mountain River Engineering, and the CAS Key Laboratory of Mountain Hazards and Earth's Surface Process. The authors are very grateful to two anonymous reviewers for insightful and supporting comments and suggestions for improving English.

Appendix A. Additional figures solicited by the reviewers to describe in more details about wave shapers and strain gauges, respectively

See Figs. A1 and A2.

References

Awaji, H., Sato, S., 1979. Diametral compressive testing method. Journal of Engineering Material and Technology 101, 139–147.

Buchar, J., Rolc, S., 2006. Dynamic fracture of ceramics. Journal de Physique IV 134, 681–686.

Frew, D.J., Forrestal, M.J., Chen, W., 2001. A split Hopkinson pressure bar technique to determine compressive stress–strain data for rock materials. Experimental Mechanics 41 (1), 40–46.

Frew, D.J., Forrestal, M.J., Chen, W., 2005. Pulse shaping techniques for testing elastic-plastic materials with a split Hopkinson pressure bar. Experimental Mechanics 45 (2), 186–195.

Gama, B.A., Lopatnikov, S.L., Gillespie Jr., J.W., 2004. Hopkinson bar experimental technique: a critical review. Applied Mechanics Review 57 (4), 223–250.

Gomez, J.T., Shukla, A., Sharma, A., 2001. Static and dynamic behavior of concrete and granite in tension with damage. Theoretical and Applied Fracture Mechanics 36, 37–49.

Gomez, J.T., Shukla, A., Sharma, A., 2002. Photoelastic evaluation of stress fields and fracture during dynamic splitting experiments. ASTM Journal of Testing and Evaluation 30 (3), 186–196.

Grantham, S.G., Siviour, C.R., Proud, W.G., Field, J.E., 2004. High-strain rate Brazilian testing of an explosive simulant using speckle metrology. Measurement Science and Technology 15, 1867–1870.

ISRM, Suggested methods for determining tensile strength of rock materials, International Journal of Rock Mechanics and Mining Sciences & Geomechanics Abstract, 1978, 15, 99–103.

Kolsky, H., 1949. An investigation of the mechanical properties of materials at very high rates of loading. Proceedings of the Physical Society B62, 676–700.

Pan, Y., Chen, W., Song, B., 2005. Upper limit of constant strain rates in a split Hopkinson pressure bar experiment with elastic specimens. Experimental Mechanics 45 (5), 440–446.

Rodriguez, J., Navarro, C., Sanchez-Galvez, V., 1994. Splitting tests: an alternative to determine the dynamic tensile strength of ceramic materials. Journal de Physique IV 4. c8-101–c8-106.

Wang, Q.Z., Wu, L.Z., 2004. The flattened Brazilian disc specimen used for testing elastic modulus, tensile strength and fracture toughness of brittle rocks: experimental results. International Journal of Rock Mechanics and Mining Sciences 41 (3), 357–358.

Wang, Q.Z., Xing, L., 1999. Determination of fracture toughness K_{IC} by using the flattened Brazilian disk specimen for rocks. Engineering Fracture Mechanics 64, 193–201.

Wang, Q.Z., Jia, X.M., Kou, S.Q., Zhang, Z.X., Lindqvist, P.-A., 2004. The flattened Brazilian disc specimen used for testing elastic modulus, tensile strength and fracture toughness of brittle rocks: analytical and numerical results. International Journal of Rock Mechanics and Mining Sciences 41 (2), 245–253.

Wang, Q.Z., Li, W., Song, X.L., 2006. A method for testing dynamic tensile strength and elastic modulus of rock materials using SHPB. Pure and Applied Geophysics 163, 1091–1100.